Moroccan Journal of Chemistry
ISSN: 2351-812X
http://revues.imist.ma/?journal=morjchem&page=login
Iaich & al. / Mor. J. Chem. 9 N°2 (2021) 185-197

Elaboration and characterization of low cost tubular ceramic supports made of Moroccan clay for microfiltration and ultrafiltration membranes

S. Iaich[(a)]*, Y. Miyah[(b)], L. Messaoudi[(c)]

[(a)] Research Team of Energy and Sustainable Development, Higher School of Technology, Guelmim, University Ibn Zohr, Agadir, Morocco.
[(b)] Laboratory of Catalysis, Materials and Environment, School of Technology, University Sidi Mohammed Ben Abdellah Fez, Morocco.
[(c)] Department of Chemistry, Materials, Membranes and Processes of Separation Team, Faculty of Sciences Moulay Ismail University, Meknes, Morocco.

** Corresponding author:*
s.iaich@uiz.ac.ma
Received °6 0ct 2020,
Revised 03 Jan 2021,
Accepted 13 Feb 2021

Abstract

The target of this study is the preparation of ceramic supports with tubular configuration of a good quality. In this case, we used local clay from Meknes area as a basic material and solid waste from wood industry as an agent of porosity because they are cheap and available. Percentages of wood powder used in the preparation of clay pastes to extrude the supports are 0, 5 and 10 % (w/w). Consequently, analysis of findings shows that the elaborated supports are in a good sintering state and are chemically very resistant. Besides, porosity and mechanical resistance increase with the addition of wood powder. Moreover, values in permeation flux increases with both the function of the final sintering temperature and the percentage of the added wood powder.

Keywords: *Clay, Ceramic support, Flux, Mechanical resistance, Porosity, Sintering.*

1. Introduction

A membrane support plays foremost a mechanical role and it ensures the solidity of the whole "support-membrane". As a result, we will evolve a support structure being perfectly appropriate for this suggested treatment while assuring a high mechanical resistance to the whole "support-membrane". For this reason, the support must have a large pore volume and a controlled pore diameter allowing laying the membrane. In this respect, the industrial supports are manufactured basically from very expensive oxides such as aluminum, silicon, zirconium and titanium [1-9]. Significant efforts have been done in recent years to produce new ceramics depending on the use of low-cost materials namely: cordierite, clay and phosphate [10-15]. The development of ceramic membranes based on natural materials and some powder wastes such as fly ash was investigated by several authors [16-24]. Clays are in abundance and need lower firing temperature in comparison with metal oxide (alumina, zirconia, titania, and silica). In our previous studies, we analyzed our chemically clay by the X-ray fluorescence, which indicates the presence of a large quantity of silicon oxide (SiO_2 = 57.61 wt %) and aluminum oxide (Al_2O_3 = 16.97 wt %) [10]. Our aim in this work is to improve new tubular macro-porous ceramic supports using clay from Meknes area in Morocco. These supports have been built through extrusion followed by sintering. Additionally, we examined the supports properties in light of sintering temperatures and wood powder percentages for the sake of optimizing the preparation conditions.

2. Experimental

2.1. Localization of sample zone

The raw material used for this work is natural clay. The sample of this clay was taken from Meknes area located in the North-West of Morocco (x: 33°53′42″N; y: 5°33′17″W). The sample was crushed, ground and sieved through a sieve of 400 µm.

2.2. Preparation of tubular supports

We prepare plastic pastes from a homogeneous clay powder, and we mix the powder with both organic additive and water. For this reason, the organic additive used in this study is wood powder because of its availability in large quantities (solid waste from the wood industry) and it is less costly compared to other additives (starch, etc.). Further, the added wood powder is easily degradable under the action of the temperature and it facilitates obtaining a clearer porosity after firing. Figure 1 shows the different steps of the preparation process of the ceramic supports. Furthermore, we formulated tests of this work by changing percentage of wood powder, volume of water, duration of mixing, malaxing and aging of the paste. Table 1 displays the optimal formulations of pastes for the preparation of tubular ceramic supports based on the clay studied. Moreover, the humid tubes have been cutted to different lengths and we left them in the open air to dry for a sufficient time. After being dried, we heat-treated the supports in an electric oven according to a thermal program for the final consolidation. The thermal program we choose is as follows (figure 2). Finally, the obtained supports have been named according to the percentage of the added wood powder (SX: S is the support and X is the percentage by weight of the wood powder). Hence, all the tubes prepared are sintered at 800 °C, 900 °C and 1000 °C and the final sintering time is 3 hours.

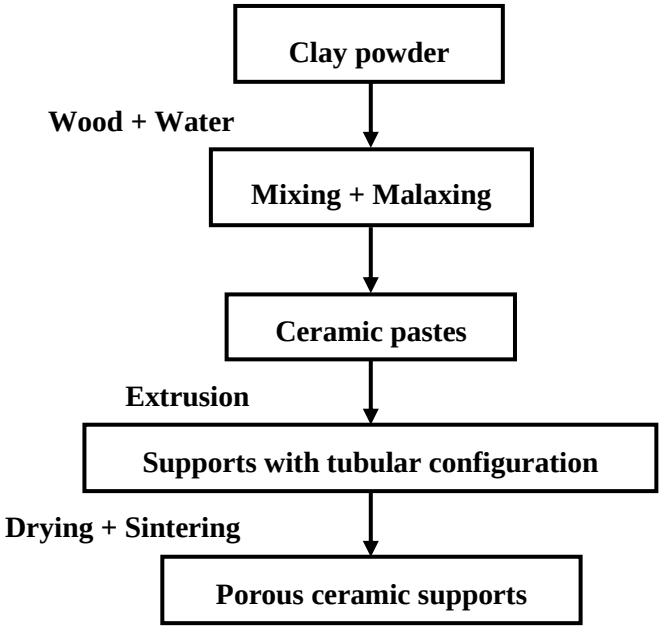

Figure 1. Stages of the preparation of porous tubular ceramic supports through extrusion method.

Table 1. Formulations prepared (PX: clay paste of X % by weight of wood powder).

Formulations	**P0**	**P5**	**P10**
Mixing time (min)	0	5	10
Malaxing time (min)	10	10	15
Volume of water (ml/Kg)	245	260	285
Aging time (h)	72	>72	>72

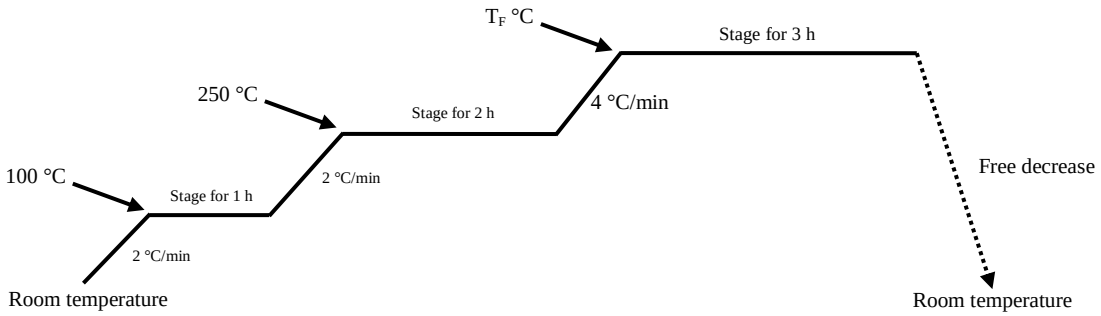

Figure 2. Sintering temperature program used for the tubular supports.

2.3. Micro-structural analysis

The characterization of the supports (surface quality, thickness) was done by scanning electron microscopy SEM (FEI QUANTA 200 U.S.A.).

2.4. Test of porosity

The porosity measurement was carried out by standard test method (ASTM C373-88).

2.5. Mechanical resistance

The compression test consists of subjecting a test specimen; a rectangular section (9 cm x 3 cm x 3 cm) prepared in the laboratory and placed between the platens of a press to two opposing axial forces. In this respect, the compression test is primarily used to determine the breaking stress of fragile materials which are difficult to be machined to a tensile test. The constraint of the rupture (σ) of specimens was determined using the standard equation:

$$\sigma = \frac{F}{S} \qquad (1)$$

Where σ is the constraint of the rupture (MPa), F is the intensity of the applied force (N) and S is the surface (mm^2).

2.6. Chemical resistance

The chemical resistant of supports was evaluated by weight loss in HNO_3 solution (1 and 0.3 N) and NaOH solution (1 and 0.3 N). The weight loss is calculated in (%) according to the following equation:

$$\%\ \text{Weight loss} = \frac{m_0 - m_1}{m_0} \times 100 = \frac{\Delta m}{m_0} \times 100 \qquad (2)$$

Where m_0 is the mass of sample before the chemical attack (g), m_1 is the mass of sample after the chemical attack (g) and $\Delta m/m_0$ is the weight loss (%).

2.7. Filtration test

The supports elaborated present tubular configuration with a length of 170 mm and an internal diameter of about 18 mm. The water permeation measurements were achieved on a filtration pilot plant in the laboratory using drinking water (figure 3).

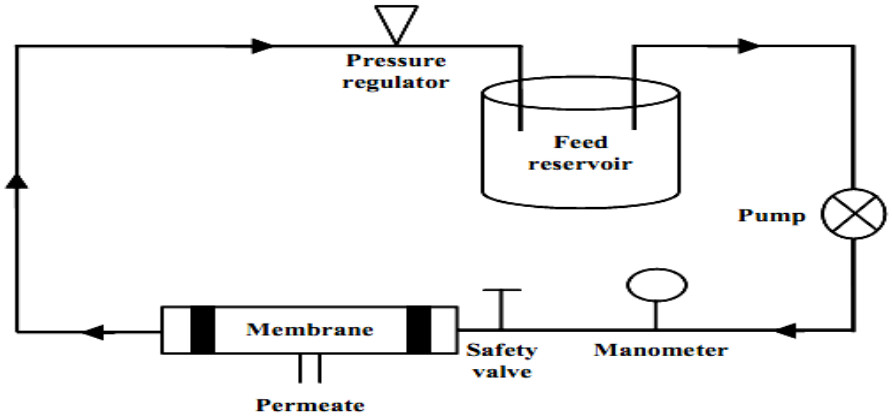

Figure 3. Scheme of pilot plant used for filtration.

All filtration experiments are conducted at a temperature of 25 °C. Permeability is calculated by tracing the flux versus time (F = f (t)), final sintering temperature (F = f (T_F)) and versus percentage of the porosity agent (F = f (PA)). Permeation flux of the support was determined using standard equation:

$$F = \frac{V}{t.S} \qquad (3)$$

Where F is the flux (L/h m^2), V is the Volume (L), t is the Time (h) and S is the filtering surface (m^2).
The filtering surface is calculated as follows:

$$S = 2.\pi.r.L = \pi.D_{int}.L \qquad (4)$$

Where π is the 3.14, D_{int} is the internal diameter of the support (m) and L is the Length of the support used (m).

3. Results and discussion

3.1. Scanning electron microscopy

The observation by scanning electron microscopy of the surface morphology and cross section of support fired at 800 °C, 900 °C and at 1000 °C during three hours (see figures 4 to 11) shows that:

- A good improvement of sintering with the increase of temperature treatment.
- The diameters of pores increase with both the final sintering temperature and the rate of the added organic [25].
- The pore volume increases with the addition of wood powder.
- A decrease in the porosity of 800 °C to 1000 °C will be confirmed subsequently by studying water porosity [11, 26].

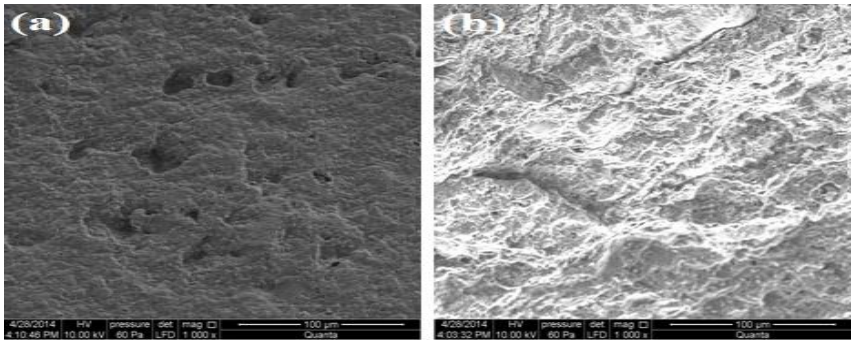

Figure 4. SEM images of the support S0 treated at 800 °C/3h, ((a): view of the surface and (b): view of the cross section).

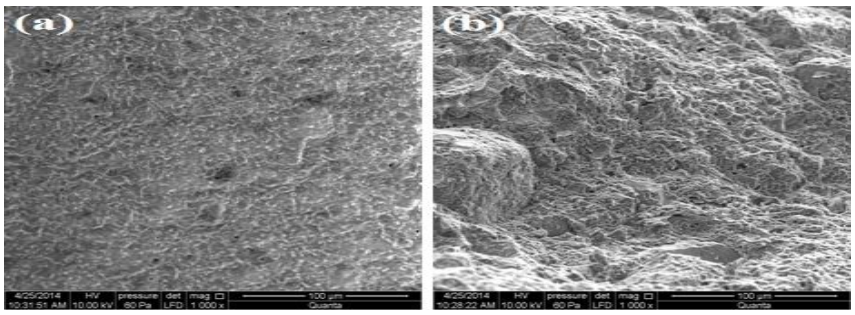

Figure 5. SEM images of the support S0 treated at 1000 °C/3h, ((a): view of the surface and (b): view of the cross section).

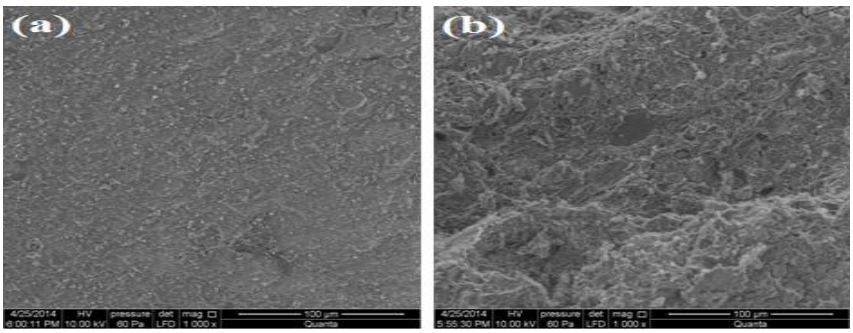

Figure 6. SEM images of the support S5 treated at 800 °C/3h, ((a): view of the surface and (b): view of the cross section)

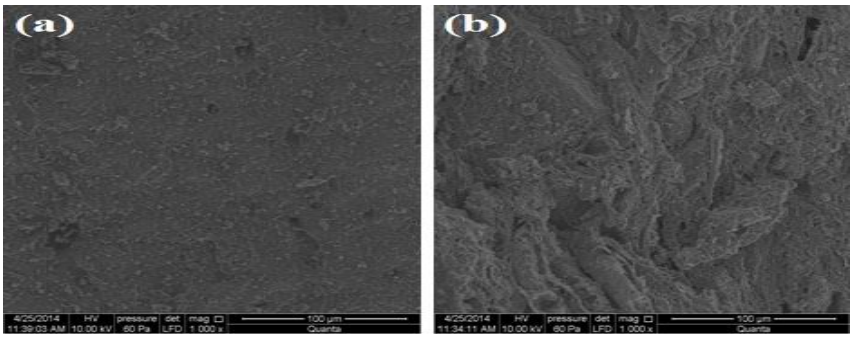

Figure 7. SEM images of the support S5 treated at 900 °C/3h, ((a): view of the surface and (b): view of the cross section).

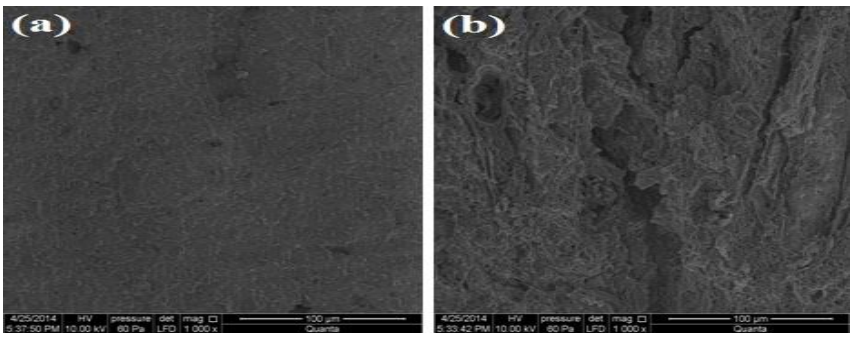

Figure 8. SEM images of the support S5 treated at 1000 °C/3h, ((a): view of the surface and (b): view of the cross section).

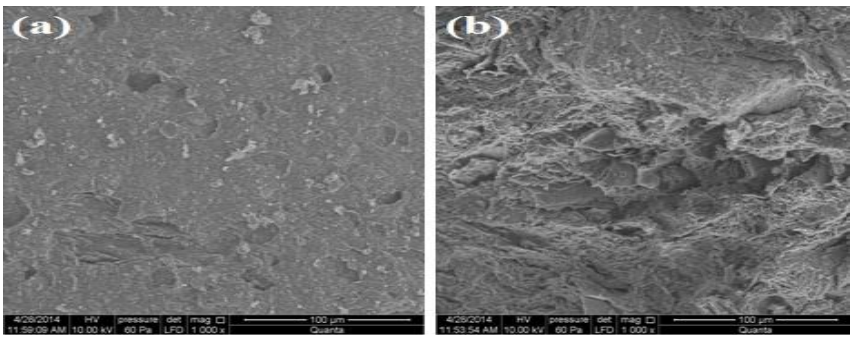

Figure 9. SEM images of the support S10 treated at 800 °C/3h, ((a): view of the surface and (b): view of the cross section).

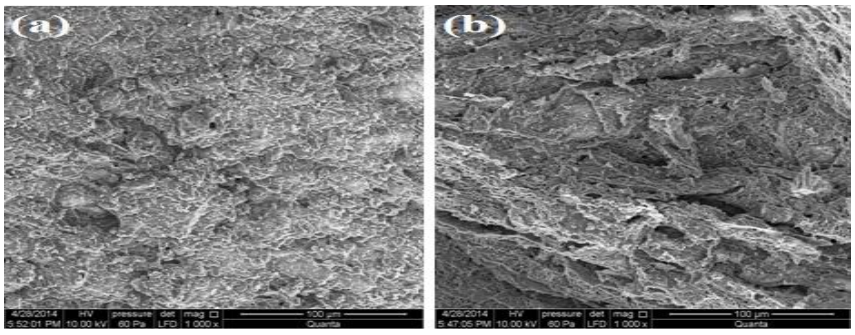

Figure 10. SEM images of the support S10 treated at à 900 °C/3h, ((a): view of the surface and (b): view of the cross section).

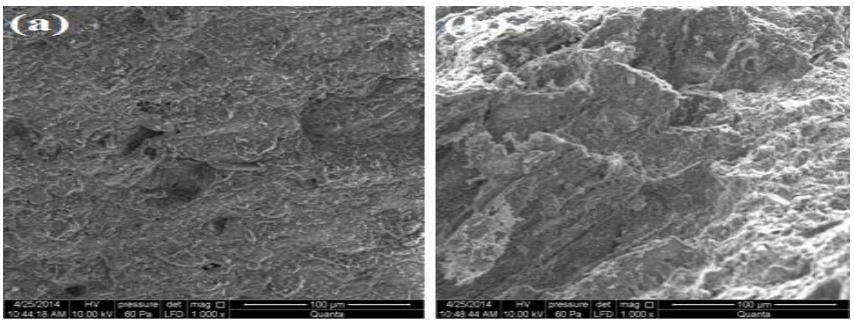

Figure 11. SEM images of the support S10 treated at 1000 °C/3h, ((a): view of the surface and (b): view of the cross section).

3.2. Porosity

Figure 12 presents the graphic representation of the ceramic supports' porosity according to the final sintering temperatures. In addition, the analysis of the results shows that the porosity decreases with the increase of the final sintering temperature and increases with the addition of added organic material (wood powder) [26-29]. In this case, it passes from 13.76 % for the supports of 0 % (S0) in weight of the organic material to be 24.6 % for the supports of 10 % (S10) in weight of the organic material treated at 900 °C/3h. Similary, the volume increases from 13.63 % for the supports 0 % (S0) of the organic material to 23.37 % for the supports 10 % (S10) of the organic material treated at 1000 °C/3h. Porosity values are very important to the lower temperatures (800 °C) for the different supports, but they display very low mechanical resistance when the sintering is not performed at this temperature [30]. Thus, this result is confirmed by the test of the mechanical resistance.

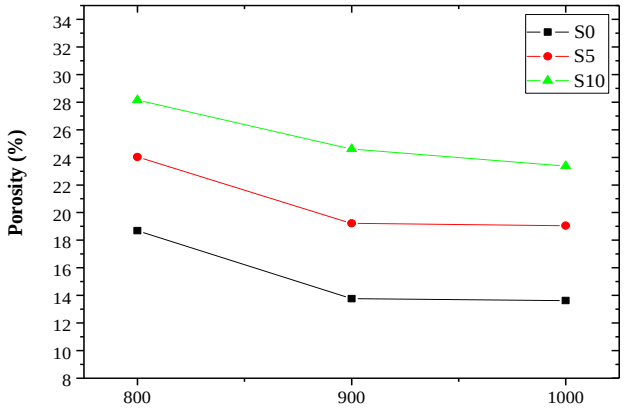

Figure 12. Porosity depending on the final sintering temperatures for the supports S0, S5 and S10.

3.3. Mechanical resistance

Figure 13 demonstrates by Megapascal (MPa) the values of the mechanical resistance of compressed specimens P0, P5 and P10 treated at different final sintering temperatures. According to the results obtained, the mechanical resistance evolves with the increase of the final sintering temperature and with the introduction of wood powder [26-30]. Values of the mechanical resistance indicate that the sintering is better with higher temperatures. Consequently, the ceramic sintered at 1000 °C for 3 hours is mechanically stronger (R_{P0} = 1.92 MPa; R_{P5} = 1.94 MPa and R_{P10} = 1.97 MPa for P0, P5 and P10 respectively).

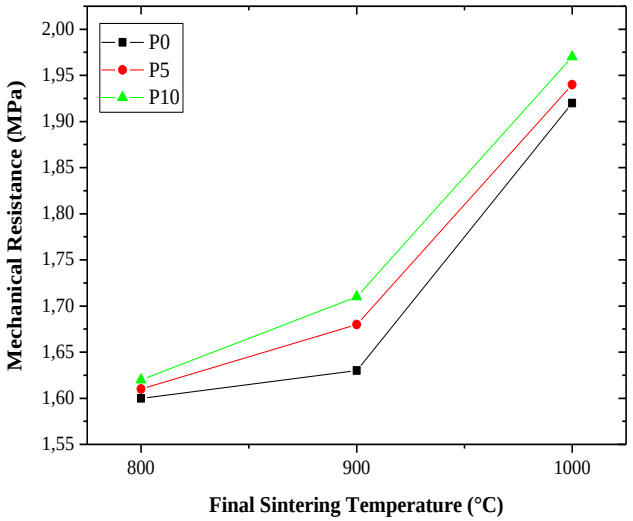

Figure 13. Evolution of the mechanical resistance of the specimens P0, P5 and P10 in different final sintering temperatures.

3.4. Chemical resistance

To estimate chemical resistance of the ceramic support, tests were performed in acidic and basic medium by sinking samples for 24 hours into baths of HNO_3 (1 and 0.3 N) and NaOH (1 and 0.3 N) at a temperature of 25 °C [26]. The results of the chemical attack for the different supports are shown in figures 14 to 16.

The test of the chemical resistance shows that the chemical attack is very significant when the solutions are highly acidic. Thus, the weight loss varies from 1.05 % to 2.50 % for the acid attack and varies from 0.13 % to 1.57 % for the basic attack for all supports developed.

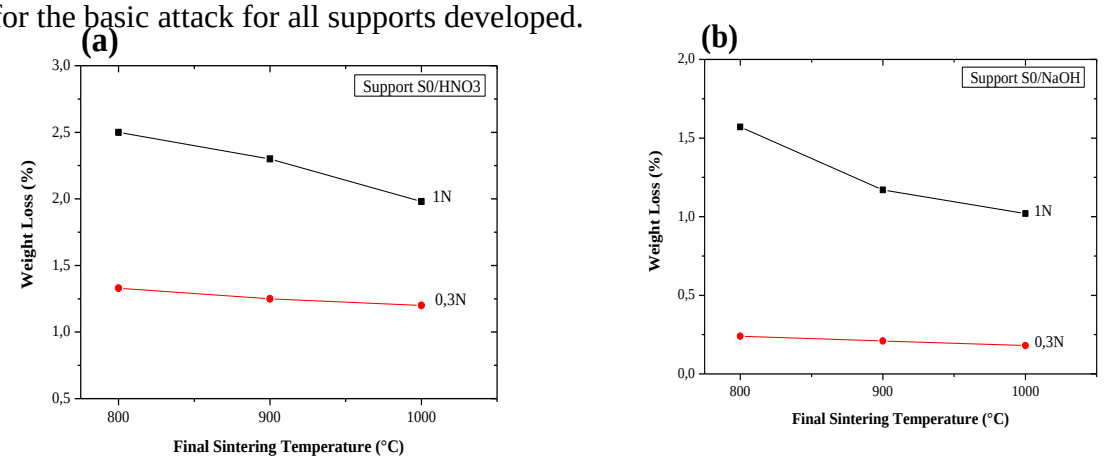

Figure 14. Variation of the weight loss of supports S0 according to the final sintering temperatures and to different concentrations of HNO_3 (a) and NaOH (b).

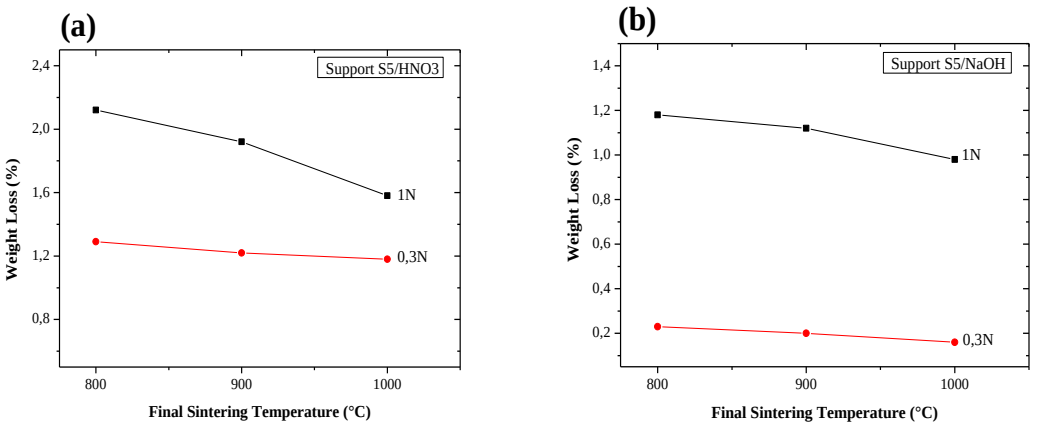

Figure 15. Variation of the weight loss of supports S5 according to the final sintering temperatures and to different concentrations of HNO_3 (a) and NaOH (b).

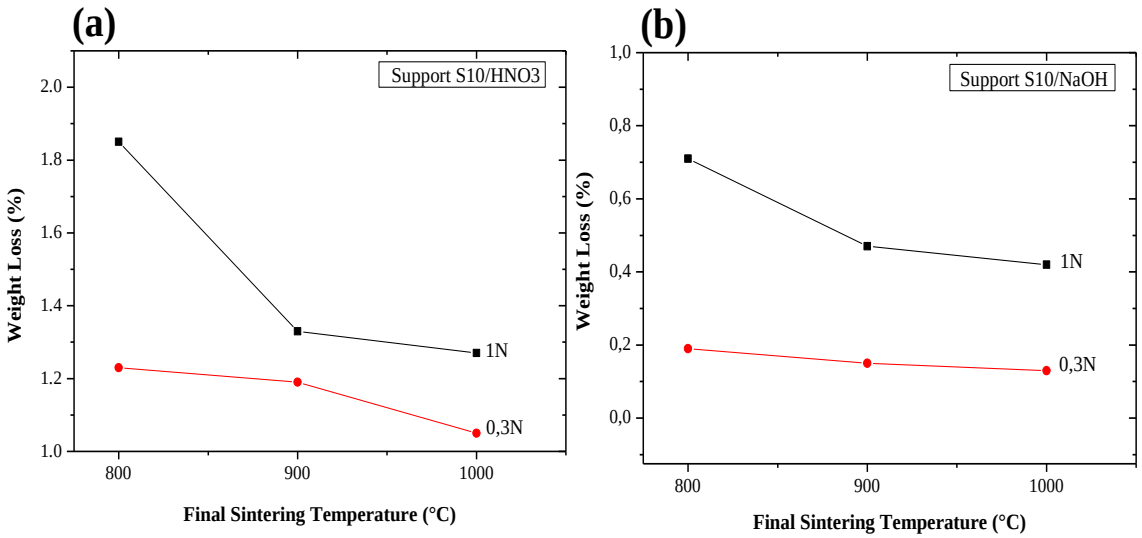

Figure 16. Variation of the weight loss of supports S10 according to the final sintering temperatures and to different concentrations of HNO_3 (a) and NaOH (b).

3.5. Filtration test

3.5.1. Variation of flux in function of time

Figure 17 to 19 shows the evolution of the flux in time of the supports S0, S5 and S10. They are treated in different final sintering temperatures with a circulation pressure of 1 and 2 bars. The analysis of the results shows that the flux values are higher of all the supports for 1 and 2 bars at the beginning of tangential filtration (for example: $F_{(S0/1000°C/2bar)}$ = 10.4 L/h.m^2 (figure 17) ; $F_{(S5/1000°C/1bar)}$ = 124 L/h.m^2 (figure 18a) ; $F_{(S5/1000°C/2bar)}$ = 499 L/h.m^2 (figure 18b) ; $F_{(S10/900°C/1bar)}$ = 249 L/h.m^2 (figure 19a) ; $F_{(S10/900°C/2bar)}$ = 499 L/h.m^2 (figure 19b)). Then, we have observed a decrease in the flux in time. This decrease is due to the partial blockage of the pores by suspended matter or traces of colloids existing in the used drinking water. After some minutes of filtration we observed stabilization of the flux, (for example: $F_{(S0/1000°C/2bar)}$ = 8 L/h.m^2 (figure 17) ; $F_{(S5/1000°C/1bar)}$ = 83 L/h.m^2 (figure 18a) ; $F_{(S5/1000°C/2bar)}$ = 269 L/h.m^2 (figure 18b) ; $F_{(S10/900°C/1bar)}$ = 83 L/h.m^2 (figure 19a) ; $F_{(S10/900°C/2bar)}$ = 221 L/h.m^2 (figure 19b)), which is explained by the

concentration polarization phenomenon. The latter is explained by several researchers: Film and gel Models proposed respectively by Michaels and Blatt [31-32].

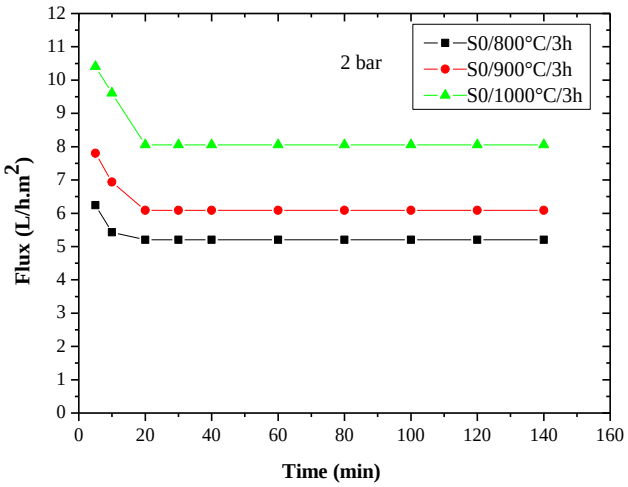

Figure 17. Evolution of the flux in function of time of the supports S0 treated at different final sintering temperatures (Pressure = 2 bar).

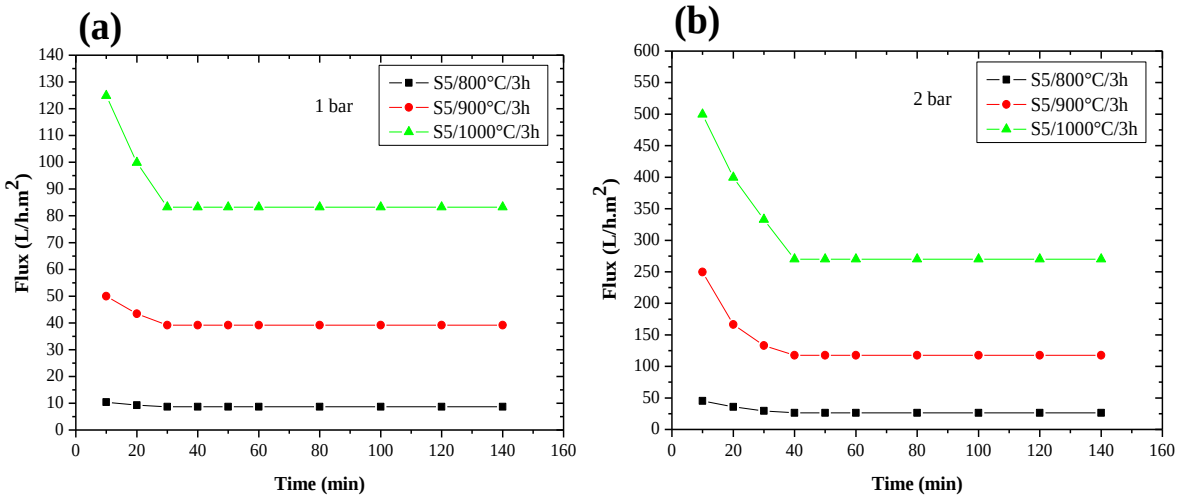

Figure 18. Evolution of the flux in function of time of the supports S5 treated at different final sintering temperatures (Pressure: 1 bar (a) and 2 bar (b)).

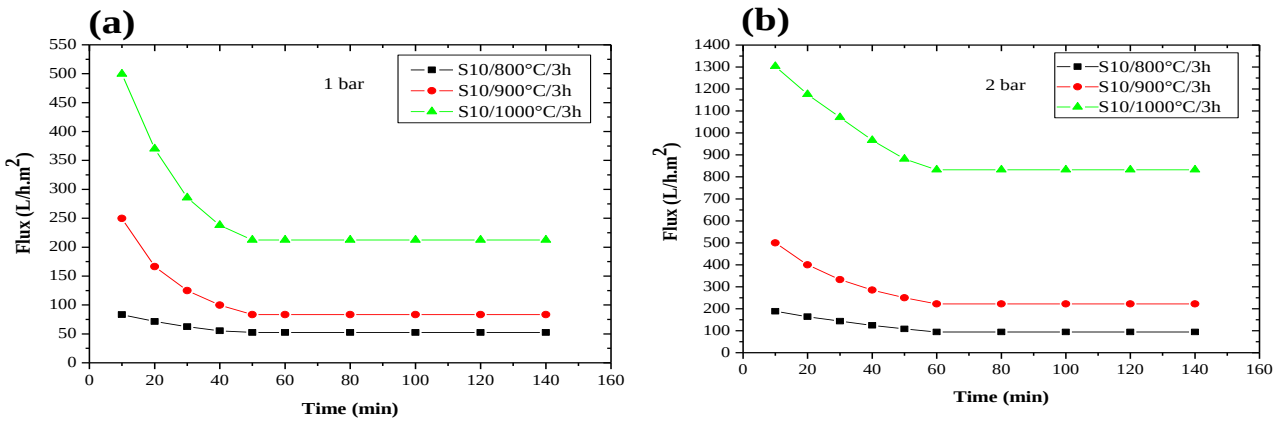

Figure 19. Evolution of the flux in function of time of the supports S10 treated at different final sintering temperatures (Pressure: 1 bar (a) and 2 bar (b)).

3.5.2. Variation of the flux in function of the final sintering temperature

Figure 20 gives a graphical representation of the evolution of the flux in function of the final sintering temperatures of the supports S0, S5 and S10 with 1 and 2 bars. The results obtained show that the flux of all the supports increases with the increase of the final sintering temperature, for instance in figure 20a, it increases from $F_{(S10/1bar)}$ = 52 L/h.m^2 for 800 °C to $F_{(S10/1bar)}$ = 212 L/h.m^2 for 1000 °C seeing that the average pore diameter of these supports increases when the sintering temperature raises.

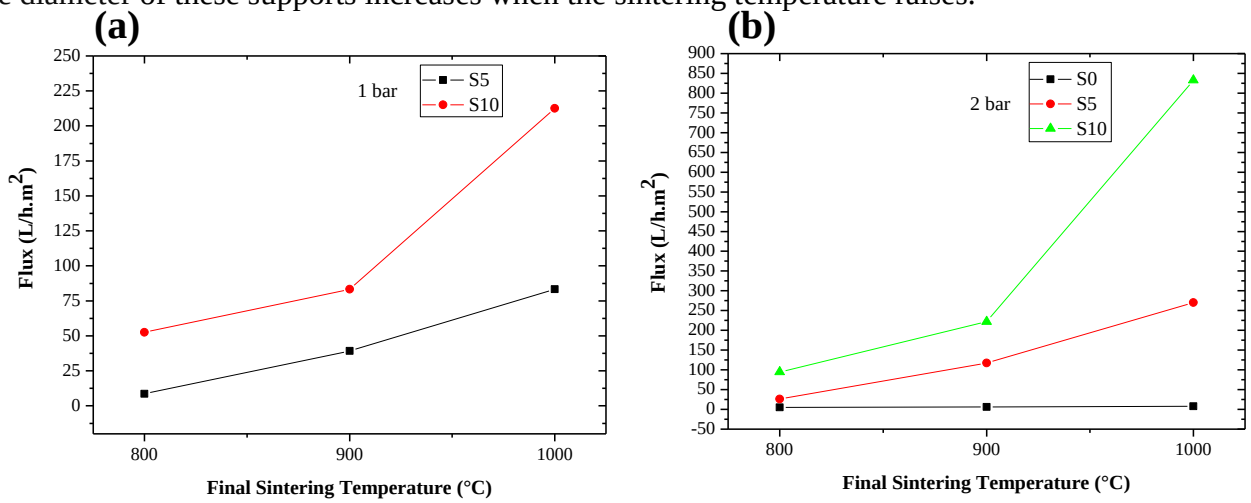

Figure 20. Variation of the flux in function of final sintering temperatures for the supports S0, S5 and S10 (Pressure: 1 bar (a) and 2 bar (b)).

3.5.3. Variation of the flux in function of the agent percentage porosity

Figure 21 shows the evolution of the flux in relation to the percentage of the added organic material (Porosity Agent) of the supports S0, S5 and S10 treated with different final sintering temperatures. We noticed that the flux values increases with the rise in the percentage of the added organic material. As a case in point, in figure 21b the flux values raise from $F_{(900°C/2bar)}$ = 6 L/h.m^2 for S0 to $F_{(900°C/2bar)}$ = 222 L/h.m^2 for S10 because the porosity characteristics of these supports increase in the final sintering temperature and with the organic additive [26-33].

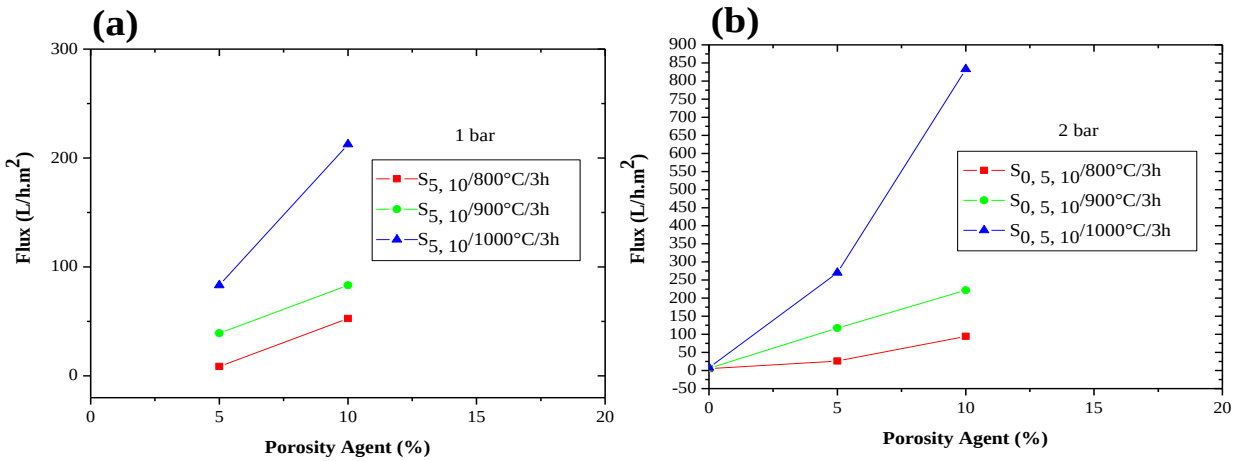

Figure 21. Flux as a function of percentage of porosity agent for the supports S0, S5 and S10 (Pressure: 1 bar (a) and 2 bar (b)).

4. Conclusions

To obtain tubular ceramic supports with very interesting final specifications and low cost, we used a natural and abundant raw material, the Moroccan clay. This clay was used as basic material for the preparation of these supports. We have elaborated ceramic supports without organic additions (S0) unfortunately the final characteristics obtained are not responding the desired goal. For this reason, we have been working instead with the wood powder as an organic additive as it is cheaper and available. The results of the characteristics of the supports are:

- A good improvement of sintering in relation to the temperature.
- The diameters of pores increase with the percentage of organic additions and also with the final sintering temperature.
- The porosity increases with the addition of wood powder.
- The mechanical resistance also increases with the addition of the wood powder and the evolution of the final sintering temperature.
- The chemical attack is very important when the solutions are highly acidic and almost null in case of basic solutions.
- The flux values grow with the rise of the final sintering temperature and with the percentage of added wood powder.
- The flux values obtained of the supports made without adding organic (S0) are very low and almost null due to the maximum densification and low porosity for every final sintering temperature (800 °C, 900 °C and 1000 °C).

In the coming works, we will focus our work on the development of new formulations of ceramic supports for microfiltration and ultrafiltration membranes from other clay materials and other organic additives with low cost.

Acknowledgments

Authors of this work express their sincere thanks to all those who participated in the realization of this present article; especially the technicians of the University Regional Interface Center (URIC) at the High School of Technology of Fez-Morocco, for analysis of Scanning Electron Microscopy (SEM). Also the Director of the Engineering office and Technology-LABOROUTE of Meknes, for tests of mechanical resistance.

References

[1] S.M. Doke, G.D. Yadav, *Clean Technol. Environ*, 8 (1) (2016) 139–149.

[2] Y. Miyah, A. Lahrichi, R. Kachkoul, G. El Mouhri, M. Idrissi, S. Iaich, F. Zerrouq, *Arab Journal of Basic and Applied Sciences*, 27 (01) (2020) 248–258.

[3] C.R. Del, C.A. Fortulan, S.R. Fontes. *Int*, 37 (4) (2011) 1161–1168.

[4] H. Nagasawa, H. Shigemoto, M. Kanezashi, T. Yoshioka, T. Tsuru, *J. Membr. Sci*, 441 (2013), 45–53.

[5] C. Falamaki, Z. Khakpour, A. Aghaie, *Journal of membrane science*, 263 (1) (2005) 103–112.

[6] M. Qiu, Y. Fan, N. Xu, *Journal of Membrane Science*, 348 (2010) 252–259.

[7] F. Bouzerara, A. Harabi, B. Ghouil, N. Medjemem, B. Boudaira, S. Condom, *Procedia Eng*, 33 (2012) 278–284.

[8] Y. Pan, T. Wang, H. Sun, W. Wang, *Sep. Purif. Technol*, 89 (2012) 78–83.

[9] K.L. Yeung, J.M. Sebastian, A. Varma, *J. Membr. Sci*, 131 (1997) 9–28.

[10] S. Iaich, L. Messaoudi, *J. Mech. Civil Eng*, 11(2) (2014) 56–62.
[11] N. Saffaj, M. Persin, Y.S. Alami, A. Albizane, M. Cretin, A. Larbot. *Appl. Clay Sci*, 31(1–2) (2006), 110–119.
[12] J. Bentama, K. Ouazzani, P. Schmitz, *Desal*, 146 (1–3) (2002) 57-61.
[13] S. Rakib, M. Sghyar, M. Rafiq, A. Larbot, L. Cot, *Sep. Pur. Technol*, 25 (1–3) (2001) 385–390.
[14] I. Barrouk, Y.S. Alami, A. Kabbabi, M. Persin, A. Albizane, S. Tahiri, *J. Mater. Environ. Sci*, 6 (8) (2015) 2190–2197.
[15] A. Abourriche, A. Benhammou, Y. El hafiane, Y. Abouliatim, L. Nibou, M. Oumam, H. Hannache, M. Birot, A. Smith, *IOSR Journal of Applied Chemistry*, 8 (5) (2015) 13–21.
[16] I. Jedidi, S. Khemakhem, A. Larbot, R. Ben Amar, *Ceram. Int*, 35 (2009a) 2747–2753.
[17] I. Jedidi, S. Saïdi, S. Khemakhem, A. Larbot, N. Elloumi-Ammar, A. Fourati, A. Charfi, A. Ben Salah, R. Ben Amar, *J. Hazard. Mater*, 172 (2009b) 152–158.
[18] S. Khemakhem, A. Larbot, R. Ben Amar, *Ceram. Int*, 5 (2009) 55–61.
[19] H. Loukili, S. Alami Younssi, M. Ouammou, A. Albizane, M. Persin, A. Larbot, *Récents progrès génie procédés*, 93 (2006) 1-37.
[20] N. Saffaj, M. Persin, Alami S. Younssi, A. Albizane, M. Bouhria, H. Loukili, H. Dach, A. Larbot, *Sep. Purif. Technol*, 47 (2005a) 36–42.
[21] N. Saffaj, S. Alami Younsi, M. Persin, M. Cretin, A. Albizane, A. Larbot, *Ceram. Int*, 31 (2005b) 205–210.
[22] N. Saffaj, S. Alami Younssi, A. Albizane, A. Messouadi, M. Bouhria, M. Persin, M. Cretin, A. Larbot, *Sep. Purif. Technol*, 36 (2004a) 107–114.
[23] N. Saffaj, S. Alami Younssi, A. Albizane, A. Messouadi, M. Bouhria, M. Persin, A. Larbot, *Desalination*, 168, (2004b) 259–263.
[24] N. Saffaj, H. Loukili, S. Alami Younssi, A. Albizane, M. Bouhria, M. Persin, A. Larbot, *Desalination*, 168 (2004c) 301–306.
[25] L. Palacio, Y. Bouzerdi, M. Ouammou, A. Albizane, J. Bennazha, A. Hernandez, J. I. Calvo, *Desal*, 245 (1–3) (2009) 501–507.
[26] A. Majouli, Y.S. Alami, S. Tahiri, A. Albizane, H. Loukili, M. Belhaj, *Desal*, 277(1–3) (2011) 61–66.
[27] A. Talidi, N. Saffaj, K. El Kacemi, Y.S. Alami, A. Albizane, A. Chakir,
Sci. Stu. & Research Chem. & Chem. Eng. Biotechnol. Food Ind, 12(3) (2011) 263–268.
[28] S. Jana, M.K. Purkait, K. Mohanty, *Appl. Clay Sci.*, 47 (3–4) (2010) 317–324.
[29] A. Harabi, A. Guechi, S. Condom, *Procedia Eng*., 33 (2012) 220–224.
[30] L. Messaoudi, A. Larbot, M. Rafiq, L. Cot, *Ceram. Glass Ind*, 910 (1995) 831–835.
[31] A.S. Michaels, "New separation technique for the CPI," *Chem. Eng. Prog*, 64 (1968) 31-43.
[32] W.F. Blatt, A. David, S. Michaels, L. Nelson, *Member. Sci. Technol*, (1970) 47–67.
[33] S. Iaich, L. Messaoudi, *J. Mater. Environ. Sci*, 5(6) (2014) 1808–1815.